Chemical Engineering Journal 155 (2009) 736–743

Contents lists available at ScienceDirect

Chemical Engineering Journal

journal homepage: www.elsevier.com/locate/cej

Pervaporation dehydration of C_2–C_4 alcohols by 6FDA-ODA-NDA/Ultem® dual-layer hollow fiber membranes with enhanced separation performance and swelling resistance

Natalia Widjojo [a], Tai-Shung Chung [a,*]

[a] Department of Chemical and Biomolecular Engineering, National University of Singapore, 10 Kent Ridge Crescent, Singapore 117602, Singapore

ARTICLE INFO

Article history:
Received 8 July 2009
Received in revised form 6 September 2009
Accepted 8 September 2009

Keywords:
Dual-layer hollow fiber membranes
Pervaporation
Alcohol dehydration
Separation factor
Flux

ABSTRACT

A novel copoly(4,4′-diphenyleneoxide/1,5-napthalene-2,2′-bis (3,4-dicarboxyl phenyl) hexa fluoro propane diimide) 6FDA-ODA-NDA/Ultem® 1010 dual-layer hollow fiber membrane for pervaporation dehydration has been fabricated via co-extrusion process. Not only can it achieve impressive alcohol dehydration performance without any post-treatment but also it particularly minimizes the membrane's swelling behavior towards aqueous alcohol solution. For isopropanol, n-butanol and t-butanol dehydrations of 85/15 (alcohol/water) wt.% feed solutions, the 6FDA-ODA-NDA/Ultem® 1010 dual-layer hollow fiber membrane can successfully attain permeate containing more than 99.7 wt.% water with considerably high flux which implies to a distinctive separation factor of the respective alcohol system. The outstanding dehydration performance of 6FDA-ODA-NDA/Ultem® 1010 dual-layer hollow fiber membranes on various aqueous alcohol feeds can be attributed to: (1) a precise formulation of the outer- and inner-layer dope compositions; (2) the size of *d*-space created in the outer-layer is a good match for size exclusion mechanism in the alcohol dehydration systems; (3) a relatively low water uptake and less swelling characteristics of the Ultem® 1010 polyimide as a supporting layer. By adjusting spinning parameters, i.e. outer-layer dope flow rate and air gap distance, the separation performance of 6FDA-ODA-NDA/Ultem® 1010 dual-layer hollow fiber membranes can be further improved.

1. Introduction

The importance of pervaporation for alcohol dehydration has been identified as one promising technology to replace conventional separation processes such as distillation or adsorption. Besides its distinctive features such as cost-effective, high energy efficiency and environmentally benign, pervaporation using membranes can effectively break the azeotrope mixture of a low molecular weight alcohol and water which cannot be separated easily by the distillation process [1–4]. A successful pervaporation membrane for molecular-scale liquid separations must have the following performance characteristics: (1) high productivity; (2) good separation factor; (3) long-term stability. Extensive research and R&D breakthroughs are needed to meet the performance challenges.

In the early stage, significant investigations have been devoted to the development of dense homogeneous polymeric membranes for the alcohol dehydration by the pervaporation technique [5–10]. However, it precludes pervaporation membranes from further commercialization due to their low flux. In early-1980s, Gesselschaft fur Trenntechnik (GFT) invented the first commercialized high flux pervaporation membrane for ethanol dehydration, so-called composite membranes, which consists of a thin layer of cross-linked poly(vinyl alcohol) supported on a porous poly(acrylonitrile) [1]. Typically, composite membranes consist of two or more layers—a thin dense skin layer and a microporous supporting layer. The beauty of this technique is that each layer can be functionalized independently to optimize membrane separation performances with respect to flux, selectivity and stability. However, it should be taken into consideration that the microporous supporting layer of a composite membrane must present negligible resistance to mass transport [11]. Otherwise, the substrate resistance leads to lower membrane productivity [12]. As such, tailoring the microstructure of the substrate is important in achieving high performance composite membranes. Apart from the selectivity and productivity, attention must be given to the structural integrity of the composite membrane.

Compared to flat asymmetric membranes, the development of asymmetric hollow fibers for pervaporation application is more attractive because it has the following advantages: (1) a large sur-

* Corresponding author at: Department of Chemical and Biomolecular Engineering, National University of Singapore, 10 Kent Ridge Crescent, Singapore 117602, Singapore. Tel.: +65 6516 6645; fax: +65 6779 1936.
E-mail address: chencts@nus.edu.sg (T.-S. Chung).

1385-8947/$ – see front matter © 2009 Elsevier B.V. All rights reserved.
doi:10.1016/j.cej.2009.09.015

Nomenclature

d	average intersegmental distance of polymer chains was reflected by the broad peak center on each X-ray pattern (Å)
J	permeate flux (g/m^2-h)
M_{dry}	weight of dry membrane (g)
M_{wet}	weight of membrane after equilibrium sorption (g)
$x_{w,i}$	weight fraction of component i in the feed (wt.%)
$y_{w,i}$	weight fraction of component i in the permeate (wt.%)

Greek symbols

α	separation factor
λ	Cu Kα radiation wavelength at 40 kV and 30 mA (=1.54 Å)
θ	X-ray diffraction angle of the peak

face area per volume ratio; (2) a self-supporting structure; (3) a self-contained vacuum channel where a feed can be supplied from the shell side while vacuum is applied on the lumen side. Practically, the development of high performance hollow fibers is not an easy task. It is found that the separation performance of hollow fiber membranes made of various materials for aqueous ethanol or isopropanol (IPA) mixtures such as Nafion 811 [13], cellulose acetate [14], polypropylene grafted with poly(acrylic acid) [15], grafted anion-exchange polyethylene [16], cellulose acetate/chitosan [17] are not impressive and far behind those polymeric flat membranes [18] or membranes prepared from inorganic and organic/inorganic materials [19–21]. This shortfall may arise from: (1) the difficulties of fabricating asymmetric hollow fiber membrane with a thin defect-free skin layer; (2) the feed-induced swelling in pervaporation membranes; (3) the effect of concentration polarization. Nevertheless, in the recent years, the superiority of dual-layer over single-layer hollow fiber membranes has been demonstrated since the invention of the one step co-extrusion process for fabricating composite hollow fibers [22–29]. Not only does the dual-layer hollow fiber membrane have the advantages of traditional single-layer hollow fiber membranes, but it also offers more benefits as follows: (1) cost saving on the expensive functional material; (2) overcoming solvent-induced swelling, i.e. by combining a material with excellent separation performance (usually higher hydrophilicity but less swell resistance) as the selective layer and a material with superior mechanical stability and greater swelling resistance as the support layer; (3) eliminating a tedious post-treatment procedure. To achieve the aforementioned objectives, numerous engineering and design parameters should carefully be taken into consideration during the hollow fiber spinning process, such as the inner and outer dope formulations, coagulant chemistry and precipitation conditions, spinning parameters, and spinneret designs.

Our previous experiences on the dual-layer hollow fiber membrane fabrication for pervaporation illustrate the importance of proper material selection for the outer- and inner-layers as well as accurate spinning parameter design. Liu et al. fabricated P84/polyethersulfone (PES) dual-layer hollow fiber membranes for IPA dehydration [24]. They reported that the separation factor can be improved from 50 to 953 after the fibers were cross-linked by a p-xylenediamine solution for 2 h. Consequently, the total flux of fibers was reduced twice as compared to the original ones. On the other hand, in the other work by Wang et al. [25], the incorporation of Ultem® 1010 (referred as Ultem® thereafter) as inner supporting layer in Torlon/Ultem® dual-layer hollow fiber membranes shows remarkable separation performance of pervaporation for alcohol dehydration without any post-treatment, although the separation performance of Torlon single-layer hollow fibers itself are not impressive [30]. This is believed due to the distinctive swelling resistance of the Ultem® as the support layer which considerably improves the overall separation performance.

To the present, only few works have been done on the systematic study of alcohol dehydration using dual-layer hollow fiber membranes [24,25]. Fundamental understanding of the science and engineering of molecular design of dual-layer hollow fiber membranes with desired morphology and balanced physicochemical properties is urgently needed. Therefore, the objective of this work is (1) to design and fabricate copoly(4,4′-diphenyleneoxide/1,5-napthalene-2,2′-bis(3,4-dicarboxylphenyl) hexa fluoro propane diimide) (6FDA-ODA-NDA)/Ultem® dual-layer hollow fiber membranes for pervaporation dehydration of water-alcohol systems; (2) to investigate the influence of phase inversion and spinning parameters on the membrane performance; (3) to demonstrate the importance of proper material selections for the outer- and inner-layers.

It should be highlighted that polyimides (PIs) are popular materials for pervaporation dehydration of alcohols [1,7–10,24,25] because of their superior thermal, chemical and mechanical stabilities and high selectivity towards water. Thus, the 6FDA-ODA-NDA polyimide was chosen as the outer-layer material owing to its distinctive properties such as excellent thermal stability, mechanical strength, and chemical resistance in addition to a proper interstitial space (d-space = 5.77 Å). This material has been studied extensively for gas separation [31–33] because it has superior gas permeability and selectivity with a reasonable material cost. The Ultem® is selected as the inner supporting layer since it has excellent swelling resistance characteristics as compared to other polyimides. To the best of our knowledge, no study has been done on the 6FDA-ODA-NDA polymer material for pervaporation.

2. Experimental

2.1. Materials

6FDA-ODA-NDA with an inherent viscosity (IV) of 0.96 dl/g, synthesized by the chemical imidization method in our lab, was employed as the outer-layer polymer material, whereas Ultem® 1010 from GE plastics (now Sabic) was selected as the inner supporting layer. Fig. 1 shows their chemical structures. *N*-methyl pyrrolidone (NMP) (>99%) from Merck was used as the solvent for both polymeric materials. In addition, ethanol (EtOH) and tetrahydrofuran (THF) used as an additive in the outer-layer dope solution were supplied by Merck and Fisher Chemicals, respectively. Polymers were dried overnight at 120 °C under vacuum before dope preparation. EtOH, IPA, and two butanol isomers (1-butanol (1-BuOH) and tert-butanol (t-BuOH)) were used to prepare binary aqueous solutions with water concentration 15 wt.%.

2.2. Dual-layer hollow fiber membrane fabrication

The spinning procedure had been described in our previous works [23–25,32] and the spinning parameters were shown in Table 1. The dope solutions and bore-fluid were extruded at specified flow rates through a triple-orifice spinneret using three ISCO syringe pumps. A dry-jet wet-spinning process was used. The resultant fibers were immersed in the coagulation bath (i.e. water) and then transported over rollers. A take-up drum was used to collect the fibers. The as-spun dual-layer hollow fiber membranes were cut into pieces of approximately 30 cm and immersed in a clean water bath for 2 days. The fibers were solvent-exchanged by three con-

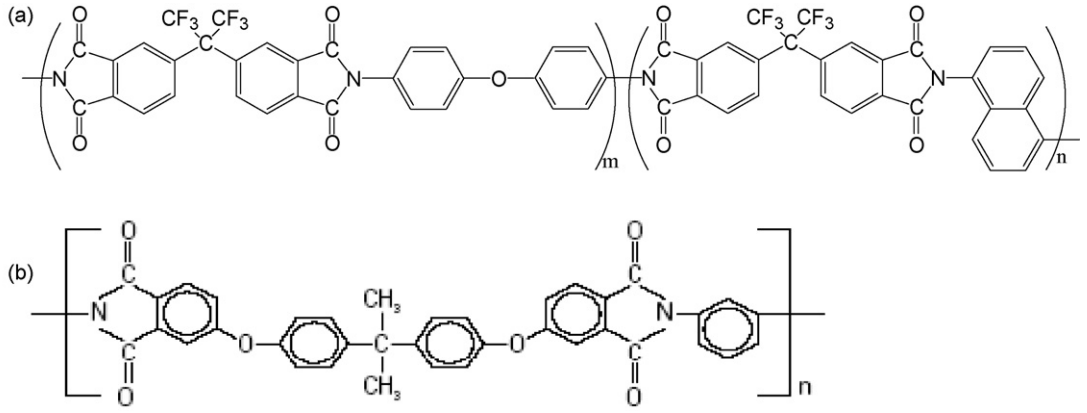

Fig. 1. Chemical structures of (a) 6FDA-ODA-NDA and (b) Ultem®.

secutive 30-min immersions in a methanol circulation. The same procedure then was repeated using n-hexane. Finally, these fibers were dried in air at ambient temperature.

2.3. SEM characterization

The morphology of the dual-layer hollow fiber membrane was observed using field emission scanning electron microscopy (FESEM JEOL JSM-6700LV) and scanning electron microscopy (SEM JEOL JSM-5600LV). The sample was fractured in liquid nitrogen and coated with platinum before FESEM or SEM analyses.

2.4. Pervaporation studies

A laboratory scale pervaporation unit was employed and the details of the apparatus have been described elsewhere [34]. For all aqueous alcohols, a feed solution of alcohol/water (85/15 wt.%) was used. It was found that the feed composition varied less than 0.5 wt.% during the entire experiment and can therefore be considered constant. The operational temperature was 60 °C. The feed flow rate was kept at 0.5 l/min for each module. The permeate pressure was maintained less than 5 mbar by a vacuum pump. Retentate and permeate samples were collected after the membrane being conditioned for about 2 h.

The flux J was determined by the mass of permeate divided by the product of the interval time and membrane area. The mass of permeate was weighed using a Mettler Toledo balance. The separation factor α is defined by the equation below:

$$\alpha = \frac{y_{w,1}/y_{w,2}}{x_{w,1}/x_{w,2}}$$

Table 1
Spinning conditions of 6FDA-ODA-NDA/Ultem® dual-layer hollow fiber membranes.

Spinning parameters	Condition
Outer-layer dope composition (6FDA-ODA-NDA/NMP/THF/EtOH)[a]	24/47/26/3
Inner-layer dope composition (Ultem®/NMP)	30/70
Outer-layer dope flow rate (ml/min)	0.3; 0.15
Inner-layer dope flow rate (ml/min)	1
Air gap (cm)	1; 5
Bore-fluid flow rate (ml/min)	0.30
Bore-fluid (NMP/water)	95/5
Coagulation bath	Water
Spinning temperature (°C)	25
Coagulation bath temperature (°C)	25
Take-up rate (m/min)	Free fall

[a] Ref. [31].

where subscripts 1 and 2 refer to alcohol and water, respectively. y_w and x_w are the weight fractions of component in the permeate and feed, and were analyzed through a Hewlett-Packard GC 6890 with a HP-INNOWAX column (packed with cross-linked polyethylene glycol) and a TCD detector. The flux and separation factor were converted to permeance and selectivity by the approach described in reference [35].

2.5. Sorption tests

Dense 6FDA-ODA-NDA membrane strips (30–60 μm) were dried under vacuum overnight. Then these pre-weighed dry membrane strips were immersed in pure DI water, EtOH, IPA, 1-BuOH and t-BuOH solutions or 85 wt.% alcohol in water solutions for 3 months, respectively [7]. The surfaces of swollen samples were blotted between tissue papers then weighed in a closed container at different time intervals. The degree of swelling was calculated from the difference between the wet weight M_{wet} after equilibrium sorption and the dry weight M_{dry}, as follows:

$$\text{degree of swelling (g/(g of dry membrane))} = \frac{M_{wet} - M_{dry}}{M_{dry}}.$$

2.6. Wide-angle X-ray diffraction (XRD)

Wide-angle X-ray diffraction (XRD) measurements of the membranes were carried out by a Shimadzu XRD-6000 X-ray diffractometer using the Cu Kα radiation wavelength (λ = 1.54 Å) at 40 kV and 30 mA. The average intersegmental distance of polymer chains was reflected by the broad peak center on each X-ray pattern. The d-space was calculated by the Bragg's equation as follows:

$$n\lambda = 2d \sin\theta$$

where θ is the X-ray diffraction angle of the peak.

3. Results and discussion

3.1. The IPA dehydration performance and basic characteristics of 6FDA-ODA-NDA and Ultem® flat sheet membranes

Table 2 displays the IPA dehydration performance of 6FDA-ODA-NDA and Ultem® flat sheet membranes. The flux of 6FDA-ODA-NDA flat membranes is about seven times higher than that of Ultem®

Table 2
Basic properties and IPA dehydration performance[a] of Ultem® and 6FDA-ODA-NDA flat dense membranes.

Polymer	Tg (°C)	Contact angle (°)	*d*-Space (Å)	Total flux (g/m^2-h)	Separation factor
6FDA-ODA-NDA	367.35	93[b]	5.36	48	276
Ultem®[c]	218	92.6	4.81	7	585

[a] Feed composition: IPA/water 85/15 wt.%; operation temperature: 60 °C.
[b] Ref. [33].
[c] Ref. [36].

ones. On the other hand, the separation factor of Ultem® flat membranes is about two times higher than that of 6FDA-ODA-NDA ones.

The 3-month sorption data of both membranes is in agreement with the isopropanol dehydration performance. The water and IPA sorption of the two dense membranes fabricated from 6FDA-ODA-NDA and Ultem® materials [36] were studied and the results are shown in Table 3. Both of these two polymer membranes have very low IPA uptake and much higher water uptake, which confirms that both two materials have high sorption selectivity towards water. For polyimide materials, hydrogen-bonding interaction generally is the predominant factor controlling the selectivity towards water in the pervaporation process due to the availability of imide groups in these materials [37].

Furthermore, it should be noted that there is a large difference in the water sorption between the aforementioned two polymer materials. 6FDA-ODA-NDA material possesses a much higher water sorption (5.3% (g/g) membrane) as compared to that of Ultem® (1.9% (g/g) membrane). In this regard, the swelling behavior of 6FDA-ODA-NDA material is more prominent than Ultem one which results in a higher flux but a lower separation factor.

From the molecular point of view, it is observed in Table 1 that Ultem® has a smaller intersegmental *d*-space, which suggests that it has a higher size and shape selectivity as compared to that of 6FDA-ODA-NDA. The relationship among free volume, *d*-space and gas permeability and solubility in gas separation [38–40] can be well correlated with the penetrant solubility and selectivity in pervaporation because both follow the solution-diffusion mechanism [25,36,41]. Thus, in addition to the *d*-space values, the gas permeabilities (O_2 and N_2) of 6FDA-ODA-NDA and Ultem® dense membranes were measured in Table 4 and their corresponding O_2 permeabilities are 6.85 barrer vs. 0.36 barrer (1 barrer = 1×10^{-10} cm^3 (STP) cm/cm^2 s cmHg) with O_2/N_2 selectivity of 5.6 and 7.5, respectively. In agreement with the *d*-space and gas permeability data, 6FDA-ODA-NDA shows a higher permeability but a lower selectivity as compared to Ultem®. This implies that the 6FDA-ODA-NDA material has a larger free volume and less rigid structure than Ultem® although the former has a much higher glass transition temperature (Tg) than the latter. In the next section, how the combination of these two materials can achieve a defect-free dual-layer hollow fiber membrane for alcohol dehydrations will be elaborated in details.

Table 3
Sorption data of 6FDA-ODA-NDA and Ultem® dense film in pure water, pure IPA and IPA/water mixtures (85/15 wt.%).

Membranes	Sorption solution	Sorption after 3 months (g/g membrane)
6FDA-ODA-NDA	Pure H_2O	0.053
	Pure IPA	No obvious change
	IPA/H_2O (85/15)	0.046
Ultem®[a]	Pure H_2O	0.019
	Pure IPA	No obvious change
	IPA/H_2O (85/15)	0.007

[a] Ref. [36].

Table 4
Gas permeation test results of 6FDA-ODA-NDA and Ultem® dense membranes.

Membranes	Permeability (barrer[a])		Permselectivity O_2/N_2
	O_2	N_2	
6FDA-ODA-NDA[b]	6.85	1.22	5.6
Ultem®[c]	0.36	0.049	7.5

[a] 1 barrer = 1×10^{-10} cm^3 (STP) cm/cm^2 s cmHg = 7.5005×10^{-18} m^2 s^{-1} Pa^{-1}; testing temperature is 35 °C.
[b] Ref. [31].
[c] Ref. [36].

3.2. Overall morphology of the as-spun dual-layer hollow fiber membranes

Fig. 2 illustrates a typical morphology of the 6FDA-ODA-NDA/Ultem® dual-layer hollow fiber membranes. At a magnification 50,000, the dual-layer fiber has a dense skin in the outer-layer which is favorable for pervaporation membranes. Both the substructures of the outer- and inner-layers of the dual-layer hollow fiber membrane are porous. The thickness of the outer-layer is less than 10 μm, while the inner supporting layer is about 25–30 μm. Moreover, the outer-layer can nicely adhere to the inner-layer without any noticeable gap in between. Practically, the delamination phenomenon in dual-layer hollow fibers can be properly controlled by the optimization of spinning parameters such as: (1) the compatibility of outer- and inner-layer materials, i.e. both 6FDA-ODA-NDA and Ultem® are polyimide materials; (2) the same solvent used in both layers; (3) the similarity in hydrophobicity of both materials, i.e. the contact angles of 6FDA-ODA-NDA and Ultem® flat membranes are 93° and 92.6°, respectively.

3.3. Comparison of IPA dehydration performance between Ultem® single-layer hollow fiber membranes and 6FDA-ODA-NDA/Ultem® dual-layer hollow fiber membranes

Table 5 summarizes the pervaporation performance of Ultem® single-layer hollow fiber membranes spun at high polymer concentrations, i.e. 32.6 and 36.8 wt.% polymer. It can be noticed that the separation factor for IPA/water system increases from 21.1 to 193 while the flux decreases from 277 to 111 g/m^2-h with an increase in polymer dope concentration. Although the dope polymer concentration has been formulated above the critical concentration of the Ultem® polymer solution (the critical concentration of Ultem® in NMP is 32 wt.% polymer [29]), the separation factor of Ultem® single-layer hollow fibers is still much lower than the intrinsic separation factor of Ultem® dense membrane (~585) [36]. This might be owing to the substructure resistance in the bulk's fiber created by the high polymer concentration in the dope solution.

In this regard, the dual-layer hollow fiber technology allows one to decrease the inner-layer polymer concentration and to reduce the substructure resistance while using a high polymer concentration in the outer-layer to obtain defect-free fibers. Compared to the Ultem® single-layer ones, the 6FDA-ODA-NDA/Ultem® dual-layer hollow fiber membranes show much higher separation performance and flux. Table 6 shows that the flux of dual-layer hollow

Table 5
IPA dehydration performance[a] of Ultem® single-layer hollow fiber membranes[b].

Ultem dope composition	Total flux (g/m^2-h)	Separation factor
32.6wt.% Ultem®	277	21.10
36.8wt.% Ultem®	111	192.47

[a] Feed composition: 87/13 wt.% (IPA/water), operation temperature: 60 °C.
[b] Spinning conditions: dope flow rate: 2 ml/min; bore-fluid: 95/5 (NMP/water); spinneret OD: 1.65 mm.

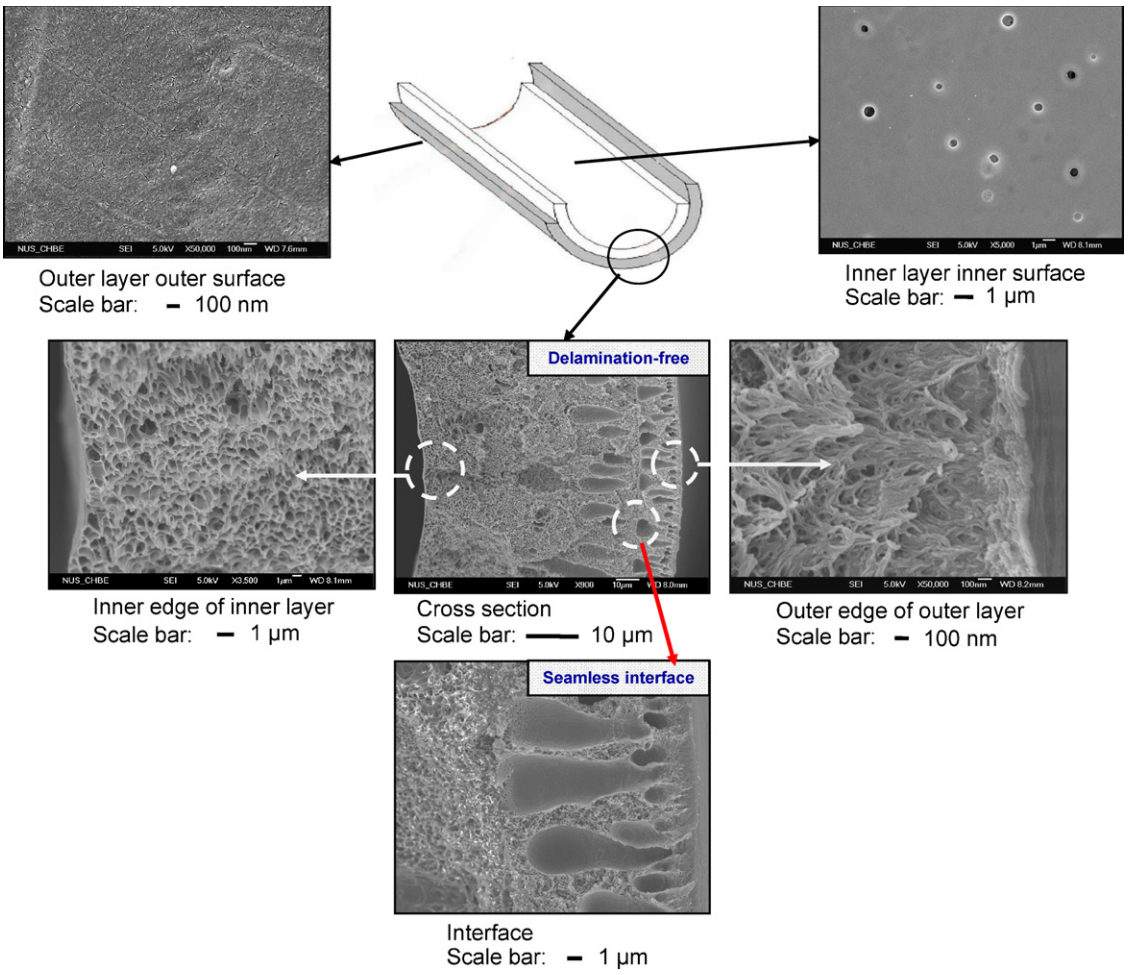

Fig. 2. SEM images of the morphology of the dual-layer hollow fiber membranes.

fibers spun at 1 cm air gap and 0.3 ml/min outer dope flow rate can reach up to 475 g/m^2-h, while the separation factor can achieve as high as 2995. A comparable performance is also shown by the dual-layer hollow fiber spun at 5 cm air gap and 0.3 ml/min outer dope flow rate. Based on this result, it is expected that the intrinsic separation factor of 6FDA-ODA-NDA should be higher than that of Ultem®. However, as discussed in Section 3.1, Table 2 displays that the separation performance of the individual flat sheet membranes is not in agreement with that of dual-layer hollow fiber ones. In fact, the separation factor of 6FDA-ODA-NDA flat sheet membranes is lower than that of Ultem® ones.

From the sorption data of both materials shown in Table 3, it can be hypothesized that the cause of this opposite phenomenon is due to the higher swelling of 6FDA-ODA-NDA material than that of Ultem®. As a result, the separation factor of 6FDA-ODA-NDA flat membranes decreases most likely due to the relatively high swelling. Therefore, the high separation performance of 6FDA-ODA-NDA material only can be revealed in the dual-layer hollow fiber membranes when Ultem® was used as the supporting layer to overcome the swelling problem. In other words, the dual-layer structure can take advantages of each material and maximize the overall membrane separation performance. The 6FDA-ODA-NDA polymer has distinctive properties such as excellent thermal stability, mechanical strength and sorption selectivity, but its superior dehydration performance can only exhibit if its supporting layer is relatively dry. Since Ultem has a very small water uptake [25] because it contains ether group which induces hydrophobicity, the inner-layer made of Ultem can minimize the overall swelling phenomenon in the dual-layer hollow fiber membrane and let 6FDA-ODA-NDA retain a high alcohol dehydration performance. Clearly, this finding highlights the superiority of dual-layer hollow fiber membranes over single-layer ones for pervaporation application since it can provide the flexibility to combine outstanding characteristics of different polymer materials.

Table 6
IPA dehydration performance[a] of 6FDA-ODA-NDA/Ultem® dual-layer hollow fiber membranes spun at different air gap distances.

Spinning ID	Outer dope flow rate (ml/min)	Air gap distance (cm)	Permeate (H_2O wt.%)	Total flux (g/m^2-h)	Separation factor
B1	0.3	1	99.84 99.77	470 480	3658 2332
B2	0.3	5	99.79 99.72	465 453	2516 1931

[a] Feed composition: 85/15 wt.% (IPA/water), operation temperature: 60 °C.

Table 7
Alcohol dehydration performances[a] of 6FDA-ODA-NDA/Ultem® dual-layer hollow fiber membranes spun at 5 cm air gap distance and 0.3 ml/min outer dope flow rate.

Spinning ID	Feed composition	Permeate (H_2O wt.%)	Total flux (g/m^2-h)	Separation factor
A2	EtOH/water = 85/15 (wt.%)	96.61	464	200.27
		94.76	493	123.99
B2	IPA/water = 85/15 (wt.%)	99.79	465	2516
		99.72	453	1931
C2	1-BuOH/water = 85/15 (wt.%)	99.77	391	2518
		99.73	376	2014
D2	t-BuOH/water = 85/15 (wt.%)	>99.99	389	>56,000
		>99.99	392	>56,000

[a] Operation temperature: 60 °C.

Table 8
EtOH dehydration performances[a] of 6FDA-ODA-NDA/Ultem® dual-layer hollow fiber membranes spun at different air gap distances and outer dope flow rates.

Sample ID	Outer dope flow rate (ml/min)	Air gap distance (cm)	Permeate (H_2O wt.%)	Total flux (g/m^2-h)	Separation factor
A0	0.1	1	94.78	587	125.08
			94.65	552	120.70
A1	0.3	1	92.51	578	85.55
			92.30	471	93.81
A2	0.3	5	96.61	464	200.27
			94.76	493	123.99

[a] Feed composition: 85/15 wt.% (EtOH/water), operation temperature: 60 °C.

3.4. The effects of different feed compositions on the dehydration performance of 6FDA-ODA-NDA/Ultem® dual-layer hollow fiber membranes

Pervaporation dehydration of four aqueous alcohol systems has been carried out using 6FDA-ODA-NDA/Ultem® dual-layer hollow fiber membranes spun at 5 cm air gap distance and 0.3 ml/min outer-layer dope flow rate. Table 7 reveals that the fabricated dual-layer hollow fiber membranes show an outstanding dehydration performance especially for isopropanol and butanols aqueous systems. Its separation performance for isopropanol and butanols systems is comparable to the previous study on Torlon/Ultem® dual-layer hollow fiber membranes [25]. However, the separation performance of 6FDA-ODA-NDA/Ultem® dual-layer hollow fiber membranes for ethanol dehydration outperforms that of Torlon/Ultem® dual-layer ones.

Table 7 shows that the order of flux in the 6FDA-ODA-NDA/Ultem® dual-layer hollow fiber membranes is: EtOH > IPA > 1-BuOH = t-BuOH, while the order of separation factor is: t-BuOH > 1-BuOH => IPA > EtOH. Based on the results, it reveals that the order of flux and separation factor is based on the ranking of alcohol molecule size and radius of gyration which described in details on the work by Wang et al. [25]. This indicates that a larger alcohol molecule size leads to a lower flux and a higher separation factor as compared to those of smaller one.

Furthermore, the 3-month sorption characterization on the 6FDA-ODA-NDA flat sheet membranes in the various alcohol solutions was conducted. Since the sorption of 6FDA-ODA-NDA dense membranes in the alcohol series cannot be measured quantitatively, XRD was used to characterize the *d*-space. *d*-Space indirectly represents the membrane's swelling behavior through the size of free volume elements or cavities formed by the random thermally motion of the flexible polymer chains before and after sorption [36]. Fig. 3 describes that the *d*-space of 6FDA-ODA-NDA flat sheet membranes measured after 3-months of sorption in different alcohol solutions (EtOH, IPA, 1-BuOH, and t-BuOH) is in agreement with the order of flux and selectivity of dual-layer hollow fiber membranes. In conclusion, a smaller *d*-space in the membranes refers to a lower sorption which results in a higher selectivity towards water and a lower total flux.

3.5. The effect of outer-layer dope flow rate and air gap distance on the ethanol dehydration performance of 6FDA-ODA-NDA/Ultem® dual-layer hollow fiber membranes

In this section, the EtOH dehydration system was undertaken since its dehydration performance manifests relatively lower separation factor (<300) and water permeation (<99 wt.%) as compared to those of higher alcohol dehydration systems. This is because the water permeation in a higher alcohol dehydration system, i.e. IPA and 1-BuOH, can reach 99.5 wt.% and above. Thus, additional efforts were given to explore whether we can improve the separation performance and investigate the effect of spinning parameter variation on the dehydration performance, i.e. outer-layer dope flow rate or air gap distance.

Table 8 displays the effects of outer-layer dope flow rate on the EtOH/water dehydration performance of 6FDA-NDA-ODA/Ultem® dual-layer hollow fibers spun at an air gap of 1 cm. It can be found that both flux and separation factor decreases with increasing outer-layer dope flow rate from 0.1 to 0.3 ml/min. The thicker outer thickness induced by a higher dope flow rate may create a higher substructure resistance that are unfavorable for both flux and separation factor [42].

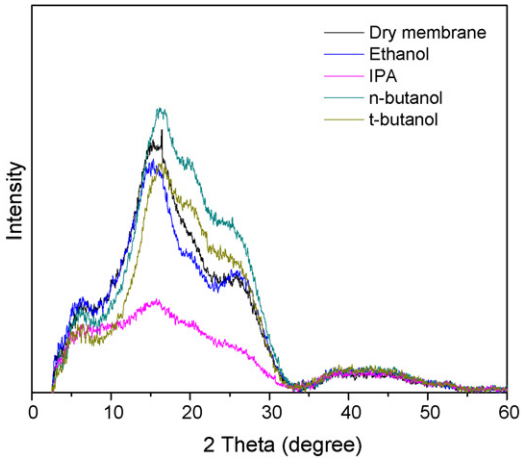

6FDA-ODA-NDA dense membrane	d-space (Å)
(a) Dry membrane	5.36
(b) Immersed in ethanol	5.76
(c) Immersed in IPA	5.62
(d) Immersed in n-butanol	5.48
(e) Immersed in t-butanol	5.40

Fig. 3. Comparison of XRD spectra of 6FDA-ODA-NDA dense membranes before and after immersion in water, EtOH, IPA, 1-BuOH, and t-BuOH, respectively.

Table 8 shows the effects of air gap distance on the dehydration performance of the EtOH/water system in the 6FDA-ODA-NDA/Ultem® dual-layer hollow fiber membranes. The flux decreases while the separation factor increases with an increase in air gap distance from 1 to 5 cm. There are two coupling mechanisms that possibly influence the enhanced separation factor with increasing air gap distance, namely: (1) the increasing amount of solvent (THF) and non-solvent (EtOH) evaporations from the outer-layer dope solution forms less defective outer skin layer; (2) the outer-layer experiences a greater elongational stress which results in a better molecular chain orientation and leads to a tighter skin structure [43,44]. Clearly, there is a trade-off between separation factor and flux to be taken into account in order to select an optimal outer-layer dope flow rate and air gap distance.

4. Conclusions

The superiority of 6FDA-ODA-NDA/Ultem® dual-layer hollow fiber membranes for a series of alcohol dehydration systems has been demonstrated in this work. Not only can it achieve outstanding alcohol dehydration performance but also it particularly minimizes swelling behavior towards aqueous alcohol solution via a proper choice of outer- and inner-layer materials. Based on the alcohol dehydration results and characterizations, the following conclusions can be drawn:

1. Compared to the Ultem® single-layer hollow fiber, the newly developed 6FDA-ODA-NDA/Ultem® dual-layer hollow fiber membrane exhibits much higher alcohol dehydration performances most likely due to reduced substructure resistance and high performance functionalized outer-layer.
2. The outstanding dehydration performance of 6FDA-ODA-NDA/Ultem® dual-layer hollow fiber membranes on various aqueous alcohol feeds, i.e. EtOH, IPA, 1-BuOH, and t-BuOH, can be attributed to: (1) a precise formulation of the outer- and inner-layer dope compositions; (2) the size of *d*-space created in the outer-layer is a good match for size exclusion in the alcohol dehydration systems; (3) a relatively low water uptake and less swelling characteristics of the Ultem® as a supporting layer.
3. By adjusting spinning parameters, i.e. outer-layer dope flow rate and air gap distance, the separation performance of 6FDA-ODA-NDA/Ultem® dual-layer hollow fiber membranes can be further improved.

Acknowledgement

The author would like to thank NUS and A-Star for funding this work with the grants of R-398-000-044-305 (NUS) and 092 139 0033 (A-Star). Thanks are also due to Dr. L.Y. Jiang for her contribution on the IPA dehydration performance of Ultem single-layer hollow fibers and Dr. Y. Liu for the 6FDA polyimide. Special appreciation is also due to Ms. Y. Wang and Dr. M.M. Teoh for their useful comments and suggestions in this study.

References

[1] X. Feng, R.Y.M. Huang, Liquid separation by membrane pervaporation: a review, Ind. Eng. Chem. Res. 26 (1997) 1048.
[2] P. Shao, R.Y.M. Huang, Polymeric membrane pervaporation, J. Membr. Sci. 287 (2007) 162.
[3] L.M. Vane, A review of pervaporation for product recovery from biomass fermentation processes, J. Chem. Technol. Biotechnol. 80 (2005) 603.
[4] Y. Huang, R.W. Baker, Bioethanol production using pervaporation and vapour permeation membranes, in: Presentation at International Congress on Membrane and Membrane Process, Honolulu, USA, July, 2008.
[5] M. Yoshikawa, A. Higuchi, M. Ishikawa, M.D. Guiver, G.P. Robertson, Vapor permeation of aqueous 2-propanol solutions through gelatin/Torlon(R) poly(amide imide) blended membranes, J. Membr. Sci. 243 (2004) 89.
[6] R.S. Veerapur, K.B. Gudasi, T.M. Aminabhavi, Pervaporation dehydration of isopropanol using blend membranes of chitosan and hydroxypropyl cellulose, J. Membr. Sci. 304 (2007) 102.
[7] X. Qiao, T.S. Chung, Fundamental characteristics of sorption, swelling, and permeation of P84 co-polyimide membrane for pervaporation dehydration of alcohols, Ind. Eng. Chem. Res. 44 (2005) 8938.
[8] L.Y. Jiang, T.S. Chung, R. Rajagopalan, Matrimid/MgO mixed matrix membranes for pervaporation, AIChE J. 53 (2007) 1745.
[9] A. Higuchi, M. Yoshikawa, M.D. Guiver, G.P. Robertson, Vapor permeation and pervaporation of aqueous 2-propanol solutions through the Torlon poly(amide imide) membrane, Sep. Sci. Technol. 40 (2005) 2697.
[10] X. Qiao, T.S. Chung, K.P. Pramoda, Fabrication and characterization of BTDATDI/MDI (P84) co-polyimide membranes for the pervaporation dehydration of isopropanol, J. Membr. Sci. 264 (2005) 176.
[11] G.H. Koops, J.A.M. Nolten, M.H.V. Mulder, C.A. Smolders, Poly(vinyl chloride) polyacrylonirile composite membranes for the dehydration of acetic acid, J. Membr. Sci. 81 (1993) 57.
[12] I. Pinnau, W.J. Koros, Relationship between substructure resistance and gas separation properties of the defect-free integrally skinned asymmetric membranes, Ind. Eng. Chem. Res. 30 (1991) 1837.
[13] I. Cabasso, Z.Z. Liu, T. Makenzie, The permselectivity of ion-exchange membranes non-electrolyte liquid mixtures. II. The effect counterions (separation of alcohol/water mixtures with nafion membranes), J. Membr. Sci 28 (1986) 109.
[14] D.R. Seok, S.G. Kang, S.T. Hwang, Use of pervaporation for separation azeotropic mixtures using two different hollow fiber membranes, J. Membr. Sci. 33 (1987) 71.
[15] Z.K. Zu, Q.W. Dai, Z.M. Liu, R.Q. Kou, Y.Y. Xu, Microporous polypropylene hollow fiber membranes. Part II. Pervaporation separation of water/ethanol mixtures by the poly(acrylic acid) grafted membranes, J. Membr. Sci. 214 (2003) 71.
[16] W. Kujawski, S.R. Krajewski, Sweeping gas pervaporation with hollow fiber ion-exchange membranes, Desalination 162 (2004) 129.
[17] H.A. Tsai, H.C. Chen, W.L. Chou, K.R. Lee, M.C. Yang, J.Y. Lai, Pervaporation of water/alcohol mixtures through chitosan/cellulose acetate composite hollow fiber membranes, J. Appl. Polym. Sci. 94 (2004) 1562.
[18] T.G. Lizon, Y.S. Ho, L.F.D. Santos, Comparative study of commercially available polymeric and microporous silica membranes for the dehydration of IPA/water mixtures by pervaporation/vapour permeation, Desalination 149 (2002) 3.
[19] M.Y. Kariduganavar, A.A. Kittur, S.S. Kulkarni, K. Rameshb, Development of novel pervaporation membranes for the separation of water-isopropanol mixtures using sodium alginate and NaY zeolite, J. Membr. Sci. 238 (2004) 165.
[20] D. Shah, K. Kissick, A. Ghorpade, R. Hannahb, D. Bhattacharyya, Pervaporation of alcohol–water and dimethylformamide–water mixtures using hydrophilic zeolite NaA membranes: mechanisms and experimental results, J. Membr. Sci. 179 (2000) 185.
[21] A. Huang, Y.S. Lin, W. Yang, Synthesis and properties of A-type zeolite membranes by secondary growth method with vacuum seeding, J. Membr. Sci. 245 (2004) 41.
[22] D.F. Li, T.S. Chung, R. Wang, Morphological aspects and structure control of dual-layer asymmetric hollow fiber membranes formed by a simultaneous co-extrusion approach, J. Membr. Sci. 243 (2004) 53.
[23] Y. Li, C. Cao, T.S. Chung, K.P. Pramoda, Fabrication of dual-layer polyethersulfone (PES) hollow fiber membranes with an ultrathin dense selective layer for gas separation, J. Membr. Sci. 245 (2004) 53.
[24] R.X. Liu, X.Y. Qiao, T.S. Chung, Dual-layer P84/polyethersulfone hollow fibers for pervaporation dehydration of isopropanol, J. Membr. Sci. 294 (2007) 103.
[25] Y. Wang, S.H. Goh, T.S. Chung, Polyamide-imide/polyetherimide dual-layer hollow fiber membranes for pervaporation dehydration of C_1–C_4 alcohols, J. Membr. Sci. 326 (2009) 222.
[26] C.C. Pereira, R. Nobrega, K.V. Peinemann, C.P. Borges, Hollow fiber membranes obtained by simultaneous spinning of two polymer solutions: a morphological study, J. Membr. Sci. 226 (2003) 35.
[27] D.F. Li, T.S. Chung, R. Wang, Y. Liu, Fabrication of fluoropolyimide/polyethersulfone dual layer asymmetric hollow fiber membranes for gas separation, J. Membr. Sci. 198 (2002) 211.
[28] L.Y. Jiang, T.S. Chung, D.F. Li, C. Cao, S. Kulprathipanja, Fabrication of matrimid/polyethersulfone dual-layer hollow fiber membranes for gas separation, J. Membr. Sci. 240 (2004) 91.
[29] N. Widjojo, T.S. Chung, W.B. Krantz, A morphological and structural study on Ultem/P84 copolyimide dual-layer hollow fiber membranes with delamination-free morphology, J. Membr. Sci. 294 (2007) 132.
[30] M.M. Teoh, T.S. Chung, K.Y. Wang, M.D. Guiver, Exploring Torlon/P84 copolyamide-imide blended hollow fiber and their chemical cross-linking modifications for pervaporation dehydration of isopropanol, Sep. Purif. Technol. 61 (2008) 404.
[31] J.Z. Ren, R. Wang, T.S. Chung, D.F. Li, Y. Liu, The effects of chemical modifications on morphology and performance of 6FDA-ODA-NDA hollow fiber membranes for CO_2/CH_4 separation, J. Membr. Sci. 222 (2003) 133.
[32] N. Widjojo, S.D. Zhang, T.S. Chung, Y. Liu, Enhanced gas separation performance of dual-layer hollow fiber membranes via substructure resistance reduction using mixed matrix materials, J. Membr. Sci. 306 (2007) 147.
[33] B.T. Low, Y. Xiao, T.S. Chung, Y. Liu, Simultaneous occurrence of chemical grafting, cross-linking, and etching on the surface of polyimide mem-

branes and their impact on H_2/CO_2 separation, Macromolecules 41 (2008) 1297.
[34] R.X. Liu, X. Qiao, T.S. Chung, The development of high performance P84 copolyimide hollow fibers for pervaporation dehydration of isopropanol, Chem. Eng. Sci. 60 (2005) 6674.
[35] W.F. Guo, T.S. Chung, T. Matsuura, R. Wang, Y. Liu, Pervaporation study of water and tert-butanol mixtures, J. Appl. Polym. Sci. 91 (2004) 4082.
[36] Y. Wang, L.Y. Jiang, T. Matsuura, T.S. Chung, S.H. Goh, Investigation of the fundamental differences between polyamide-imide (PAI) and polyetherimide (PEI) membranes for isopropanol dehydration via pervaporation, J. Membr. Sci. 318 (2008) 217.
[37] S.I. Semenova, H. Ohya, K. Soontarapa, Hydrophilic membranes for pervaporation: an analytical review, Desalination 110 (1997) 251.
[38] C. Fuhrman, M. Nutt, K. Vichtovonga, M.R. Coleman, Effect of thermal hysteresis on the gas permeation properties of 6FDA-based polyimides, J. Appl. Polym. Sci. 91 (2004) 1174.
[39] C.C. Hu, C.S. Chang, R.C. Ruaan, D.M. Wang, J.Y. Lai, Effect of free volume and sorption on membrane gas transport, J. Membr. Sci. 226 (2003) 51.
[40] L. Shao, L. Liu, S.X. Cheng, Y.D. Huang, J. Ma, Comparison of diamino cross-linking in different polyimide solutions and membranes by precipitation observation and gas transport, J. Membr. Sci. 312 (2008) 174.
[41] L.Y. Jiang, H.M. Chen, Y.C. Jean, T.S. Chung, Ultra-thin polymeric interpenetration network with enhanced separation performance approaching ceramic membranes for biofuel, AIChE J. 55 (2009) 75.
[42] T.S. Chung, X. Hu, The effect of air gap distance on the morphology and thermal properties of polyethersulfone hollow fibers, J. Appl. Polym. Sci. 66 (1997) 1067.
[43] T.S. Chung, The limitations of using Flory-Huggins equation for the states of solutions during asymmetric hollow fiber formation, J. Membr. Sci. 126 (1997), 19. T. S.
[44] T.S. Chung, S.K. Teoh, X. Hu, Formation of ultrathin high performance polyethersulfone hollow fiber membranes, J. Membr. Sci. 133 (1997) 161.